HERON contains contributions based mainly on research work performed in I.B.B.C. and STEVIN and related to strength of materials and structures and materials science.

HERON vol. 18 1972 no. 4

Contents

REALISTIC ANALYSIS OF REINFORCED CONCRETE FRAMED STRUCTURES

Ir. J. Blaauwendraad
Data Processing Division,
Structural Group, Rijkswaterstaat,
Ministry of Transport, Water Control and Public Works

REALISTIC ANALYSIS OF REINFORCED CONCRETE FRAMED STRUCTURES

Summary

A calculation of the complementary moments due to second-order effects and the analysis of the stability of reinforced concrete framed structures can be conceived as follows. With the aid of a computer a very large number of M-N-$\varkappa$ diagrams can be produced on the basis of the standard specified stress-strain diagrams for concrete and steel. A framed structure is then analysed with an available program which takes account of second-order effects. The flexural stiffnesses EI to be adopted are estimated and corrected with reference to the M-N-$\varkappa$ diagrams calculated once before and held in store for the purpose.

The present paper discusses the drawbacks of this approach and proposes a method of analysis which can be fitted into existing programs for framed structures and dispenses with the large number of stored M-N-$\varkappa$ diagrams. It is shown that direct use can be made of the stress-strain diagrams. The results are just as reliable as those obtained by the procedure utilising the M-N-$\varkappa$ diagrams.

Acknowledgments

The FORTRAN programming was carried out by Mr. H. Eimers of the Rijkswaterstaat. In testing the method of analysis we had the benefit of valuable criticism from Ir. A. K. de Groot of the TNO Institute for Building Materials and Structures. In the context of his work for Committee A 17 of the Netherlands Committee for Concrete Research (CUR) he analysed a number of structures in actual practice on the basis of the approach described in this paper. His efforts helped speedily to reveal the initial shortcomings of the method.

This paper is essentially the text of a lecture given by the author at the twice-repeated postgraduate course on "Stability of Buildings". A slightly modified version of this text will be published in the same time in the Dutch journal "CEMENT". The present English translation has been prepared by Ir. C. van Amerongen.

To end up we are greatly indebted to the editorial staff of this periodical for the given opportunity to propagate a computer oriented technique for stability search.

Realistic analysis of reinforced concrete framed structures

1 What went before?

Since 1967 there has, in the Netherlands, been animated discussion about how the stability of tall buildings can be investigated. Although the term itself is not usually employed, it is widely realised that we are here faced with a *non-linear* problem. The fact that the framed structures under consideration, composed of bar-type members, do not behave linearly is due to two causes. For one thing, the horizontal displacements become so large that the vertical loading gives rise to additional moments in the columns. This second-order effect is sometimes formally referred to as *geometric* non-linearity. The second cause is the *material* non-linearity, also known as *physical* non-linearity. Concrete cannot resist tension, and its compressive stress-strain diagram is not linear, but curved. For reinforcing steel this latter phenomenon applies both to tensile and to compressive stress. This material non-linearity is usually embodied in a moment-curvature diagram dependent on the normal force (M-N-$\varkappa$ diagram).

Since 1969 the discussion took a turn in that a more computer-oriented approach has now been adopted. This is based on Livesley's [1] publication in which he shows how second-order effects can quite simply be incorporated in the known computer programs for the analysis of framed structures in accordance with the displacement method.

The type of program in current use can indeed take account of the development of ideally plastic hinges at the ends of the members, but considers each member otherwise as a prismatic beam with constant flexural stiffness EI and extensional stiffness EA. In practice the procedure for using a program of this kind is as follows. First an estimate of the expected stiffness values EI is made, and on completion of the analysis it must be checked, with reference to the moments obtained, whether the assumption for EI was correct. To do this it is, in principle, necessary to have a large

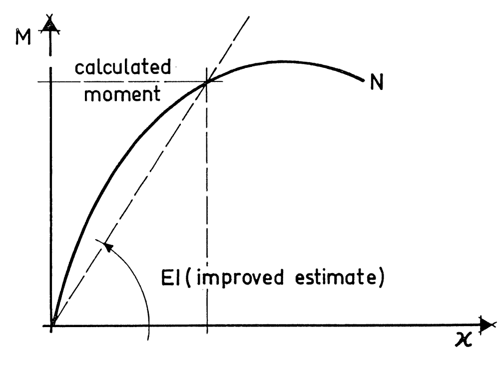

Fig. 1.
Moment-curvature diagram applicable to the calculated normal force in the member.

number of moment-curvature (M-$\varkappa$) diagrams at one's disposal (Fig. 1). If the estimate is found to have been significantly incorrect, the calculation will have to be repeated.

2 What do we need?

Estimating the stiffness

We should like to replace the procedure for correcting the flexural stiffness, as described above, by a more automated technique. The M-$\varkappa$ diagrams could perhaps be stored in the computer. The program can indeed be so arranged that it will itself seek out the corrected EI values from this collection of diagrams and repeat the calculation. However, if we consider this idea more closely, we shall soon realise that this is not the way to tackle the problem. For one thing, the number of possible diagrams is very large. We shall wish to provide a wide choice of cross-sectional shapes for the structural members, and many different systems or methods of reinforcing them. In addition, the diagram for any particular cross-sectional shape of a member must be established for a sufficiently large number of values of N. Furthermore, there remains the question of choosing the σ–ε-diagram to serve as our starting point. If it is decided in due course to adopt a modified version of this diagram, it will necessitate revising the whole set of stored M–N–$\varkappa$-diagrams.

It is these considerations that compel us to abandon the idea of storage of the diagrams. Instead, the solution to the problem must be sought in a procedure whereby that part of the moment-curvature diagram which we require at a particular stage is, at the time, rapidly regenerated in a separate subprogram. This means that for each new cross-sectional shape we shall prepare a *subroutine* of its own, here to be further referred to as "DRSN". All these subroutines are based on one and the same convention for the form in which the σ–ε-diagram is to be utilised. The part of DRSN which relates to the chosen σ–ε-diagram can therefore in turn advisably be accommodated in a separate subroutine. For reasons which will emerge in due course, the latter will be referred to as "EMOD".

With this approach the following advantages are achieved:

- For each cross-sectional shape of a structural member we have to produce one subroutine (DRSN) instead of a large number of M–$\varkappa$-diagrams. This subroutine is not dependent on the convention for the σ–ε-diagram and can therefore be utilised as long as the need to apply that cross-sectional shape exists.
- If a different σ–ε-diagram is adopted, it will be necessary merely to alter one small subroutine (EMOD) which is applicable to all cross-sectional shapes.
- This new proposal will have the effect of reducing costs, because the performance of computational operations by computer is becoming steadily cheaper. On the other hand, M–$\varkappa$-diagrams would have to be stored permanently accessible in backing stores, so that this system could be relatively expensive.
- The interchangeability between various computer centres is greatly simplified. A subroutine written in standard FORTRAN is easier to despatch than a tape or a disc with tabulated data.

Stiffness varies along member

Since we can now simply automate the procedure of estimating a new stiffness value, we should like also to obviate another imperfection in programs as mentioned in 1. It is not true that in reinforced concrete structures the flexural stiffness *EI* along one and the same member is constant. This would be so only if the bending moment acting on the member were of constant magnitude along the whole length of the latter. As a result of cracking in the tensile zone and plastification in the compressive zone the flexural stiffness is less according as the moment has a higher value. Fig. 2

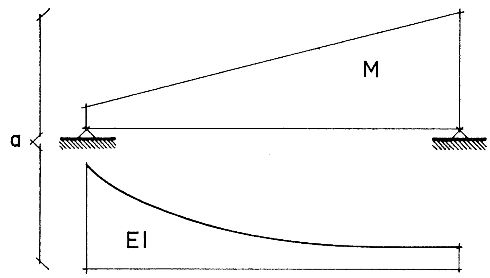

Fig. 2a.
For a linear bending moment diagram the distribution of EI is arbitrary.

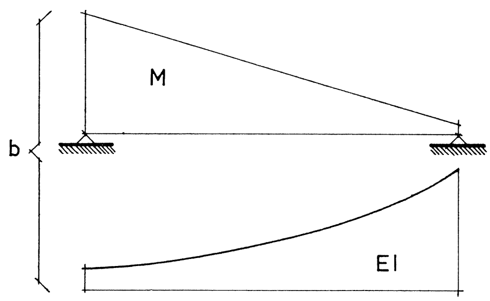

Fig. 2b.
This distribution is moreover different for a different linear bending moment diagram.

illustrates that a linear moment distribution in the member is associated with an arbitrary distribution of *EI,* which is deducible from the moment-curvature diagram in the manner represented in Fig. 1.

It will be shown that this aspect can very simply be accommodated in the existing displacement method programs.

Centroidal axis shifts

The computer programs familiarly employed in structural analysis schematise an elastic framework to a system of axes or centre-lines of members which in general intersect one another at the joints of the structure. Each such centre-line coincides with the centroidal axis of the member in question. It must not be confused with the neutral axis of the member, which (in this particular context) is the line at which zero strain occurs and which will coincide with the centroidal axis only if there is no normal force acting. The centroidal axis for a member of composite section is calculated with due regard to the different moduli of elasticity of the constituent parts.

A problem arises in circumstances where cracking and plastification are liable to occur. To illustrate this we shall consider a rectangular section provided with symmetrically arranged reinforcement (Fig. 3). An obvious choice is to choose the axis

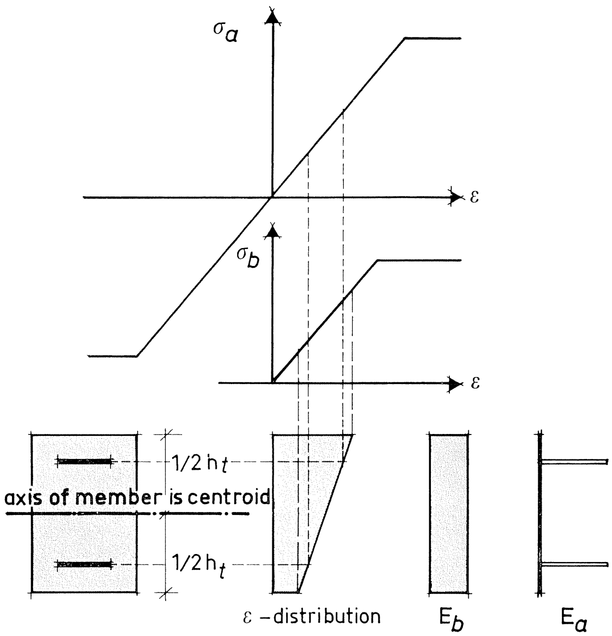

Fig. 3a.
The centroid is located on the axis of the member.

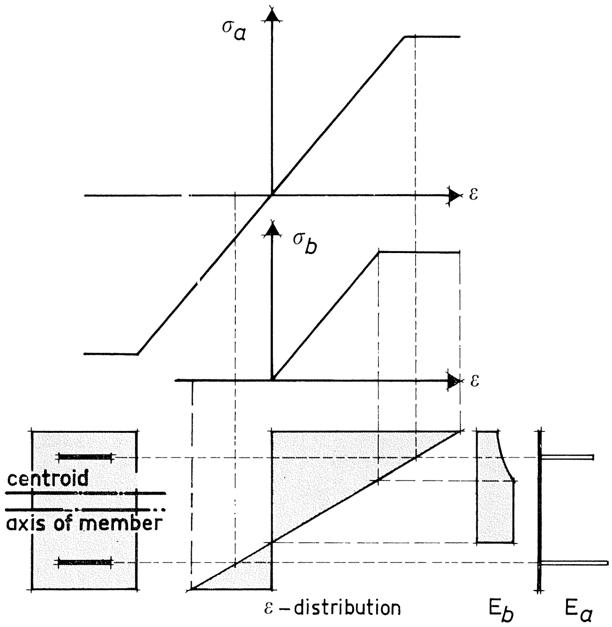

Fig. 3b.
The centroid is not located on the axis of the member.

of the member as being located at mid-depth (h_t being the depth of the section). The concrete conforms to a bilinear σ–ε-diagram which is of significance only for the compressive zone, while the reinforcing steel conforms to a two-branched σ–ε-diagram which is valid both for compression and for tension. A normal force N and a moment M act at the section. We shall now consider two possibilities. In Fig. 3a the combination of N and M has been so chosen that the whole section is in compression and the strains ε which occur are small. In that case all the concrete fibres will be located on the elastic branch of the σ_b–ε-diagram and therefore have the same modulus of elasticity E_b. The reinforcement, too, has remained elastic and its stiffness behaviour is characterised by E_a, which is the same for the top and the bottom reinforcement. For the distribution of E_b and E_a thus obtained, the centroid of the section is indeed located exactly at mid-depth. Our choice as to the position of the axis of the member was therefore correct.

Now let us consider another combination of N and M. This is so chosen that a tensile zone develops (Fig. 3b) and plastification occurs. If we again plot the strains on to the σ–ε-diagrams, we find that a new distribution of the apparent moduli E_a and E_b has been obtained. In the tensile zone E_b is zero and in the compressive zone E_b is in part constant, but in the region where yielding occurs it decreases for increasing values of the strain ε. The reinforcing steel undergoes yielding even in the compressive zone. As a result of this the apparent modulus of elasticity E_a is not of the same magnitude at top and bottom. With the distribution now obtained for E_a and E_b the centroid of the section does *not* coincide with the axis located at mid-depth of the section, i.e., for this case our choice for the position of the axis of the member was incorrect.

Since we are including the effect of the normal force N on the flexural deformation in our consideration of the problem, it is necessary correctly to describe the complementary moment due to N. The shifting of the centroidal axis must therefore be taken into account in the computer program. This, too, will be found to constitute no more than a minor intervention in the existing programs based on the displacement method.

Summary of desired features

The foregoing considerations can be summarised in the following points:

1. The existing programs which can cope with geometric non-linearity (second-order flexural deflection) must be extended to deal with material non-linearity (cracking and plastification).
2. The extension must be simple to perform in any currently used program based on the displacement method.
3. The storage of large series of M–N–$\varkappa$-diagrams must be avoided because this is too expensive and makes interchangeability more difficult.
4. Programming must be so contrived that only a minor alteration to the program is needed if it is decided to adopt a different σ–ε-diagram.

5. The variation of the flexural stiffness along the member must find expression in the calculation.
6. The shift of the centroidal axis associated with second-order flexural deflection is of importance and must therefore be taken into account in the program.

The requirements stated in points 3 and 4 can be fulfilled by a procedure whereby the information needed at any particular instant is computed at that same instant. To this end, a subroutine DRSN will have to be established for each cross-sectional shape of the structural members. The part thereof which is common to all cases, namely, the part relating to the σ–ε-diagram, is accommodated in one subroutine EMOD which is valid for all cross-sectional shapes.

3 Stiffness matrix S^e of a prismatic member in the linear theory

The analysis of a framed structure in accordance with the displacement method will always follow a scheme as envisaged in Fig. 4. In connection with the discussion of the procedure it will be assumed that the reader is familiar with the displacement method as generally applied [1], [2]. First, the stiffness matrix S^e is determined for all the individual members of the structure. This can be done with respect to a system of co-ordinate axes made to coincide with the axis of the member, and then a transformation is performed to the general system of co-ordinate axes which is adopted for the structure as a whole. In accordance with a fixed procedure these matrices S^e

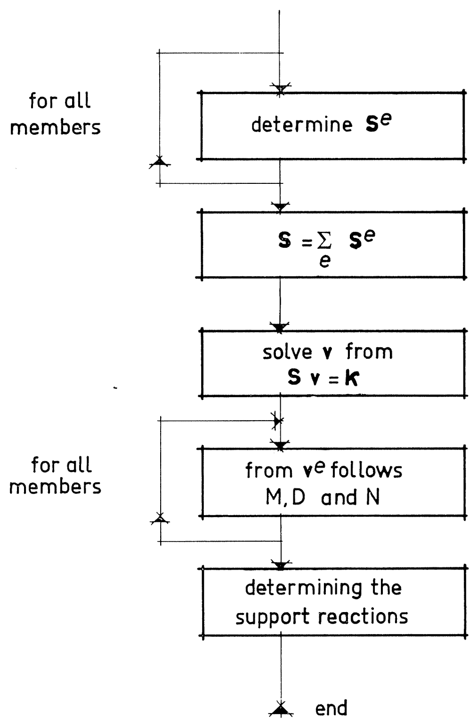

Fig. 4.
Approximate flowchart for a linear analysis of framed structures with the displacement method.

are combined into a stiffness matrix $\boldsymbol{S}$ which is valid for the overall structure. All the external loading is brought together in a vector $\boldsymbol{k}$ corresponding to $\boldsymbol{S}$. The displacements $\boldsymbol{v}$ of the joints can then be solved from the set of equations:

$$\boldsymbol{S}\boldsymbol{v} = \boldsymbol{k} \tag{1}$$

We next return to the individual member. From $\boldsymbol{v}$ we obtain the six displacements $\boldsymbol{v}^e$ of the two ends of the member, enabling us to calculate the moments M, the shear force D and the normal force N. We do this for all the members.

Except for minor extensions the scheme represented in Fig. 4, remains valid for the non-linear analysis. For the type of structures which we envisage here the taking account of the non-linear effects has consequences only in so far as the stiffness matrix $\boldsymbol{S}^e$ relating to the co-ordinate axes system for the member is concerned. This we shall more particularly consider. The other operations remain valid unchanged.

The reader will already have perceived that it is our wish to make matters as easy as possible for ourselves. We shall consider only loading applied at the joints and ignore any hinged connections that may be present or the formation of any plastic hinges. For these conditions the approach and the procedure adopted in, for example, [1] and [3] remain valid unchanged. Here we shall confine ourselves to discussing the extension with regard to those publications.

Separating the elementary deformation problem

The six-by-six matrix $\boldsymbol{S}^e$ which establishes the relationship between the six displace-

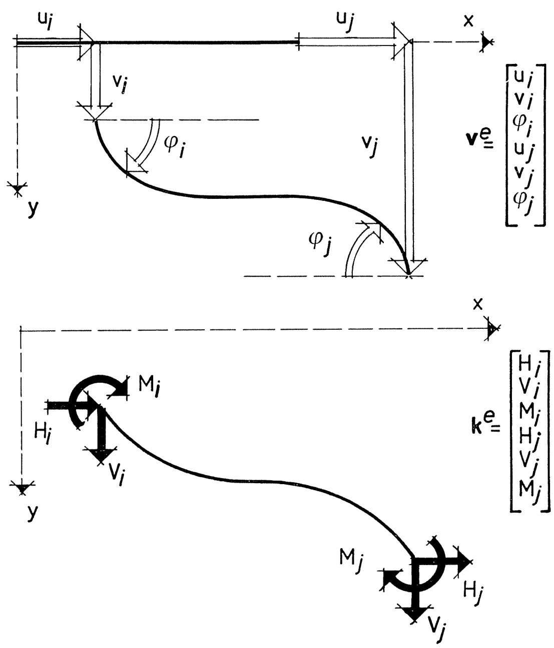

Fig. 5.
Displacements $\boldsymbol{v}^e$ and member end forces $\boldsymbol{k}^e$ in the e^{th} member.

ments $\boldsymbol{v}^e$ and the six end forces $\boldsymbol{k}^e$ in e-th member (Fig. 5) can be built up in two steps. We shall first explain this for the linear theory.

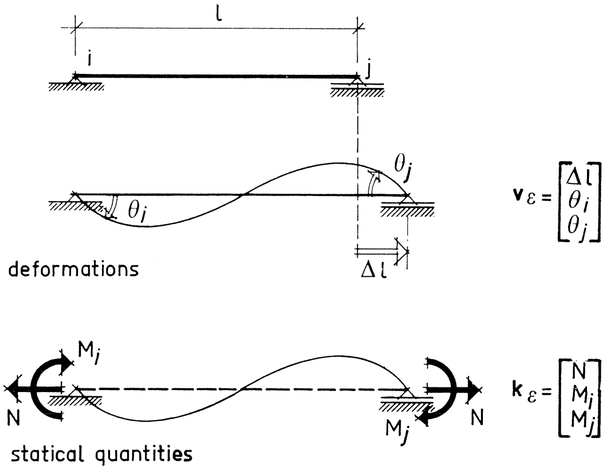

Fig. 6.
Elementary deformation problem.

The first step comprises the analysis of the elementary deformation problem of Fig. 6. The three statical quantities $\boldsymbol{k}_\varepsilon$ cause three deformations $\boldsymbol{v}_\varepsilon$. Their interrelationship can be written als:

$$\boldsymbol{S}_\varepsilon \boldsymbol{v}_\varepsilon = \boldsymbol{k}_\varepsilon \tag{2}$$

For a prismatic member this can be written out in the following form:

$$\begin{bmatrix} \frac{EA}{l} & 0 & 0 \\ 0 & \frac{4EI}{l} & \frac{2EI}{l} \\ 0 & \frac{2EI}{l} & \frac{4EI}{l} \end{bmatrix} \begin{bmatrix} \Delta l \\ \theta_i \\ \theta_j \end{bmatrix} = \begin{bmatrix} N \\ M_i \\ M_j \end{bmatrix} \tag{3}$$

We shall now perform the second step. While loading indicated in Fig. 6 continues to act, we first displace the whole member horizontally through a distance u_i, then let the support i move downwards a distance v_i, and the support j next move downwards a distance v_j. The member is then in the condition shown in Fig. 5. The displacements u_i, v_i and v_j are small in relation to the length l of the member. The linear theory presupposes that the *rigid body displacement* that has been performed has not changed the stresses in the member nor the forces at the ends thereof. From a comparison of Fig. 5 and Fig. 6 it then follows:

$$
\begin{aligned}
H_i &= -N & \Delta l &= -u_i+u_j \\
V_i &= (M_i+M_j)/l & \theta_i &= \varphi_i-(v_j-v_i)/l \\
M_i &= M_i & \theta_j &= \varphi_j-(v_j-v_i)/l \\
H_j &= +N \\
V_j &= -(M_i+M_j)/l \\
M_j &= M_j
\end{aligned}
\tag{4}
$$

On introducing the *combination matrix* $\boldsymbol{C}$ the following shorter notation for (4) can be written ($\boldsymbol{C}^T$ is the transpose of $\boldsymbol{C}$):

$$\boldsymbol{k}^e = \boldsymbol{C}^T\boldsymbol{k}_\varepsilon \qquad \boldsymbol{v}_\varepsilon = \boldsymbol{C}\boldsymbol{v}^e \tag{5}$$

where:

$$\boldsymbol{C} = \begin{bmatrix} -1 & 0 & 0 & 1 & 0 & 0 \\ 0 & 1/l & 1 & 0 & -1/l & 0 \\ 0 & 1/l & 0 & 0 & -1/l & 0 \end{bmatrix} \tag{6}$$

With the aid of (2) and (5) a relation between the six forces $\boldsymbol{k}^e$ and the six displacements $\boldsymbol{v}^e$ can be derived:

$$\boldsymbol{S}^e\boldsymbol{v}^e = \boldsymbol{k}^e \tag{7}$$

The stiffness matrix $\boldsymbol{S}^e$ is found to be simple to calculate as:

$$\boldsymbol{S}^e = \boldsymbol{C}^T\boldsymbol{S}_\varepsilon\boldsymbol{C} \tag{8}$$

Quantities neglected in the linear theory

In each of the two steps described above a simplifying approximation is made which is no longer permissible in the non-linear analysis. In the first step, the elementary deformation problem, it is assumed that the rotations θ_i and θ_j are due only to the moments M_i and M_j. They are calculated as if the normal force N were not present. If we are to include the second-order effects in our analysis, this approximation, i.e., neglecting the presence of N, can no longer be permitted. In the linear theory it is furthermore assumed that the change in length Δl is caused by the normal force alone. Strictly speaking, a correction should be applied to this if the member is additionally subjected to bending moments. The resulting deflection of the member causes its ends to move a short distance towards each other (bowing). However, for normal structures such as we are considering here, this effect is negligible even in second-order calculations.

The second step likewise involves an approximation. It is tacitly assumed that the magnitude of the bearing reactions $(M_i+M_j)/l$ remains unchanged when the member shown in Fig. 6 undergoes displacements v_i and v_j to the position shown in Fig. 5. In that case we neglect the fact that, because of the slight inclination of the member, the horizontal forces H_i and H_j will in reality produce an additional couple. In other words: the normal force N causes additional vertical reactions. To take account of these a correction $\Delta \boldsymbol{S}^n$ must be applied to $\boldsymbol{S}^e$.

Our conclusion is that two approximations, involving the neglecting of certain quantities, as adopted in the linear theory will have to be rectified:

- The flexural part of $\boldsymbol{S}_\varepsilon$ is dependent also on the normal force N.
- A correction $\Delta \boldsymbol{S}^n$ necessitated by the inclination of the member must be applied to the matrix $\boldsymbol{S}^e = \boldsymbol{C}^T \boldsymbol{S}_\varepsilon \boldsymbol{C}$

The stiffness matrix now becomes:

$$\boxed{\boldsymbol{S}^e = \boldsymbol{C}^T \boldsymbol{S}_\varepsilon \boldsymbol{C} + \Delta \boldsymbol{S}^n} \tag{9}$$

4 Stiffness matrix S^e of a prismatic member in the non-linear theory

Elementary deformation problem

We must establish a new relation between the two rotations θ_i and θ_j, on the one hand, and the two moments M_i and M_j, on the other, in a manner whereby the effect of the normal force is duly expressed. In theory this can be done in an exact manner by judiciously solving the relevant differential equation. In actual practice, however, a simple solution can be found only for prismatic members. If N is a compressive force of magnitude P, so that $N = -P$, the relationship is:

$$\begin{bmatrix} \frac{EA}{l} & 0 & 0 \\ 0 & p\frac{EI}{l} & q\frac{EI}{l} \\ 0 & q\frac{EI}{l} & p\frac{EI}{l} \end{bmatrix} \begin{bmatrix} \Delta l \\ \theta_i \\ \theta_j \end{bmatrix} = \begin{bmatrix} N \\ M_i \\ M_j \end{bmatrix} \tag{10}$$

where:

$$p = \frac{\beta \sin \beta - \beta^2 \cos \beta}{2(1-\cos \beta) - \beta(\sin \beta)}$$

$$q = \frac{\beta^2 - \beta \sin \beta}{2(1-\cos \beta) - \beta(\sin \beta)}$$

$$\beta^2 = \frac{l^2 P}{EI}$$

In the limit case where P is zero, p does indeed have the value 4 and q the value 2, so that the matrix of (3) is precisely obtained.

Correction $\Delta \boldsymbol{S}^n$

The additional vertical reactions due to the normal force N which arise in connection

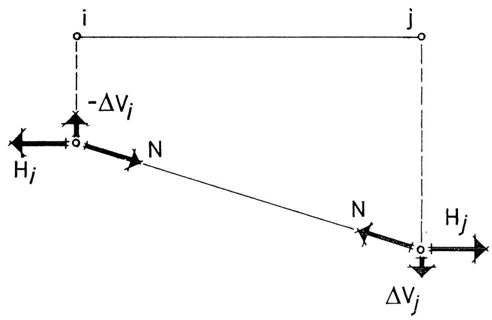

Fig. 7.
Additional vertical reactions due to the normal force N when the member is in an inclined position.

with the change in position of the member when $\boldsymbol{S}_\varepsilon$ becomes $\boldsymbol{S}^e$ are red simply from Fig. 7. Their magnitude is as follows:

$$\Delta V_i = \frac{v_i - v_j}{l} \cdot N$$

$$\Delta V_j = \frac{-v_i + v_j}{l} \cdot N$$

In matrix notation this becomes:

$$\begin{bmatrix} 0 & 0 & 0 & 0 & 0 & 0 \\ 0 & \frac{N}{l} & 0 & 0 & \frac{-N}{l} & 0 \\ 0 & 0 & 0 & 0 & 0 & 0 \\ 0 & 0 & 0 & 0 & 0 & 0 \\ 0 & \frac{-N}{l} & 0 & 0 & \frac{N}{l} & 0 \\ 0 & 0 & 0 & 0 & 0 & 0 \end{bmatrix} \begin{bmatrix} u_i \\ v_i \\ \varphi_i \\ u_j \\ v_j \\ \varphi_j \end{bmatrix} = \begin{bmatrix} 0 \\ \Delta V_i \\ 0 \\ 0 \\ \Delta V_j \\ 0 \end{bmatrix} \tag{11a}$$

or:

$$\Delta \boldsymbol{S}^n \boldsymbol{v}^e = \Delta \boldsymbol{k}^e \tag{11b}$$

Total matrix $\boldsymbol{S}^e$

If we substitute $\boldsymbol{S}_\varepsilon$ of (10) and $\Delta \boldsymbol{S}^n$ of (11) into the expression (9) for $\boldsymbol{S}^e$, putting $N = -P$, we find exactly the same stiffness matrix as previously given by Livesley in [1]. In comparison with his direct approach our treatment offers a major advantage. Of the three components $\boldsymbol{C}$, $\boldsymbol{S}_\varepsilon$ and $\Delta \boldsymbol{S}^n$ which compose the stiffness matrix $\boldsymbol{S}^e$ in (9), only $\boldsymbol{S}_\varepsilon$ is dependent on the stiffness properties of the material used. The matrix $\boldsymbol{C}$ is determined entirely by the geometric quantity l, and the matrix $\Delta \boldsymbol{S}^n$ additionally by the normal force N. *The influence of varying stiffness and a shifting centroidal axis is therefore confined to the three-by-three matrix* $\boldsymbol{S}_\varepsilon$. Only this matrix is changed when cracking and plastification (deviation from the linear σ–ε-diagram) occur. Thanks to this important conclusion we can now confine our attention to this matrix.

5 Stiffness matrix S_ε^e for a member with varying stiffness in the non-linear theory

We shall again investigate the problem of Fig. 6, but now for an elastic member with a given arbitrary distribution of the modulus of elasticity E, which may vary quite arbitrarily across the depth of the section and also in the linear direction of the member. This, in effect, is the situation that is liable to arise when cracking and plastification occur. We shall choose a *fixed axis* for the member to serve as a *reference line* which is independent of cracking and suchlike phenomena. The position of this axis can be freely chosen. In Fig. 8 it is located at mid-depth. On the other hand, the

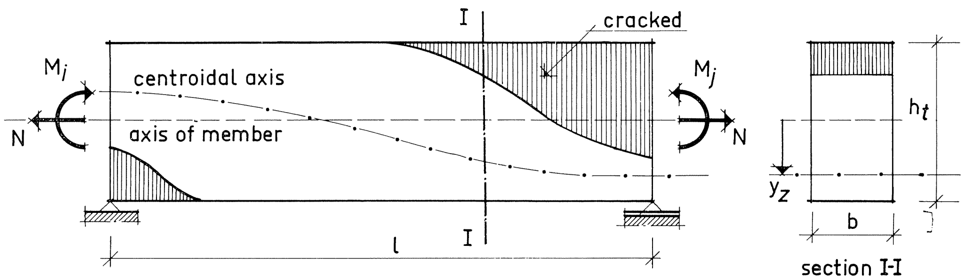

Fig. 8. Irregular distribution of the modulus elasticity as a result of plastification and cracking.

centroidal axis is determined entirely by the distribution of the modulus of elasticity E. We shall now consider a section $I-I$. From the known variation of E across the depth of the section the location of the centroid of this section can be determined. Let y_z denote the distance thereof to the chosen fixed axis.

We now choose the centroid as the origin of the vertical axis $\bar{y}$ (see Fig. 9a). The extensional stiffness EA and the flexural stiffness EI are determined by the well known standard formulas:

$$EA = b \int_{-h}^{h_t - h} E(\bar{y}) \cdot \mathrm{d}\bar{y}$$
$$EI = b \int_{-h}^{h_t - h} E(\bar{y}) \bar{y}^2 \cdot \mathrm{d}\bar{y} \qquad (13)$$

If a normal force N and a moment $\overline{M}$ are acting at the centroid, a linear strain distribution develops across the depth of the section. This strain can be separated into an average strain $\bar{\varepsilon}_g$ which is constant on the whole depth and a curvature portion which is of zero value at the centroid and has a linear distribution from $-\varkappa h$ to $\varkappa(h_t-h)$. The relation between $\bar{\varepsilon}_g$ and $\varkappa$, on the one hand, and N and $\overline{M}$, on the other, can be expressed quite simply with EA and EI:

$$\begin{bmatrix} EA & 0 \\ 0 & EI \end{bmatrix} \begin{bmatrix} \bar{\varepsilon}_g \\ \varkappa \end{bmatrix} = \begin{bmatrix} N \\ \overline{M} \end{bmatrix} \tag{14}$$

The behaviour of any section is determined by the three data y_z, EA and EI. On the basis of this information we shall now proceed to construct a stiffness matrix $\boldsymbol{S}_\varepsilon$ which is defined at the fixed axis of the member. We shall accordingly let the normal force N from the vector $\boldsymbol{k}_\varepsilon$ act at that axis. It appears that $\boldsymbol{S}_\varepsilon$ can be worked out in two ways. The first of these ties up with the *finite element method*, which is used for the analysis of slabs and plates. An assumption is made as to the distribution or pattern of the displacements. This is not a new feature in stability analysis. Van Leeuwen and Van Riel [5] utilised a sinusoidal deflected shape, even though it was known that a different shape would occur in reality. The second possibility is equally interesting in that it establishes a link-up between the analysis programs for frame-works (composed of bar-type members) and the stability analysis which Van Riel and De Groot performed with the aid of the *finite difference technique* quite some time ago [6]. In the present paper we shall more particularly be concerned with the further development of the finite element method as an approach to the problem.

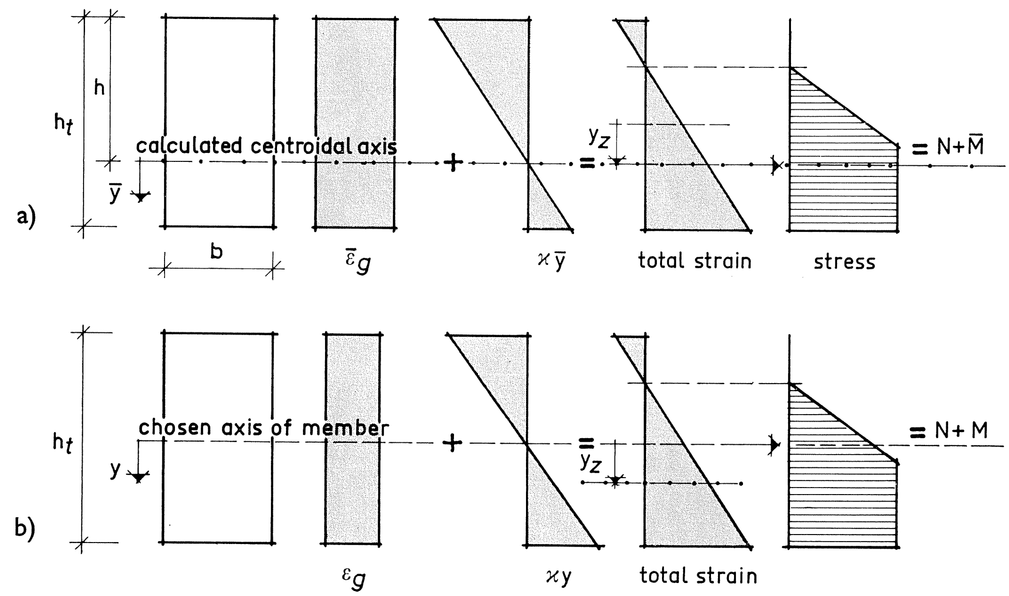

Fig. 9. Definition of average strain, curvature, normal force and bending moment at a section.

For the procedure employing the finite difference technique a short summary will be given here; for further information the reader is referred to De Groot's publication [7].

Whichever procedure is adopted, we shall base ourselves on the usual fundamental assumptions of flexural theory, namely, that plane sections remain plane (linear strain function in Fig. 9) and that normals to the axis of the member remain perpendicular thereto after application of loading (no deformation due to shear).

Method of assumed displacement field

We shall first deal with the simpler case where y_z is zero. For this case the usual approach is to assume a *linear* distribution in terms of x for the displacements $\bar{u}(x)$ in the direction of the axis of the member and to assume a *cubic* polynomial for the displacement $v(x)$ perpendicular to the axis:

$$\begin{aligned} \bar{u}(x) &= \frac{l-x}{l}\cdot\bar{u}_i + \frac{x}{l}\cdot\bar{u}_j \\ v(x) &= \frac{x(l-x)^2}{l^2}\cdot\theta_i + \frac{-x^2(l-x)}{l^2}\cdot\theta_j \end{aligned} \tag{15}$$

The strain $\bar{\varepsilon}_g$ and the curvature $\varkappa$ are:

$$\begin{aligned} \bar{\varepsilon}_g &= \frac{d\bar{u}}{\mathrm{d}x} = \frac{\bar{u}_j-\bar{u}_i}{l} = \frac{\Delta l}{l} \\ \varkappa &= -\frac{d^2v}{\mathrm{d}x^2} = \frac{4l-6x}{l^2}\cdot\theta_i + \frac{2l-6x}{l^2}\cdot\theta_j \end{aligned} \tag{16}$$

The potential energy for this member is:

$$P = \tfrac{1}{2}\left\{\int_0^l\left[EA\bar{\varepsilon}_g^2 + EI\varkappa^2 + N\left(\frac{\mathrm{d}v}{\mathrm{d}x}\right)^2\right]\mathrm{d}x - N\,\Delta l - M_i\theta_i - M_j\theta_j\right\} \tag{17}$$

The term with $\mathrm{d}v/\mathrm{d}x$ in quadratic form under the integral symbol is the second-order term in this expression. It corresponds to the work done by the normal force N in deflecting the member.

On substitution of (16) into (17) P becomes a quadratic expression comprising the three deformations Δl, θ_i and θ_j. By equating to zero the derivative of P with respect to each of these deformations we obtain three equations containing Δl, θ_i and θ_j. These equations determine the minimum for P and are written in abbreviated notation as follows:

$$\boldsymbol{S}_\varepsilon \boldsymbol{v}_\varepsilon - \boldsymbol{k}_\varepsilon = \boldsymbol{0} \tag{18}$$

So we have determined the required matrix $\boldsymbol{S}_\varepsilon$. It is found to be composed of two components:

$$\boldsymbol{S}_\varepsilon = \boldsymbol{S}_\varepsilon^0 + \boldsymbol{S}_\varepsilon^n \tag{19}$$

For these two three-by-three matrices it can readily be deduced that ($\psi = x/l$):

$$\boldsymbol{S}_\varepsilon^0 = \begin{bmatrix} \frac{1}{l}\int_0^1 EA\,\mathrm{d}\psi & 0 & 0 \\ 0 & \frac{1}{l}\int_0^1 EI(4-6\psi)^2\,\mathrm{d}\psi & \frac{1}{l}\int_0^1 EI(4-6\psi)(2-6\psi)\,\mathrm{d}\psi \\ 0 & \frac{1}{l}\int_0^1 EI(4-6\psi)(2-6\psi)\,\mathrm{d}\psi & \frac{1}{l}\int_0^1 EI(2-6\psi)\,\mathrm{d}\psi \end{bmatrix} \tag{20a}$$

$$\boldsymbol{S}_\varepsilon^n = \begin{bmatrix} 0 & 0 & 0 \\ 0 & \frac{2}{15}Nl & -\frac{1}{30}Nl \\ 0 & -\frac{1}{30}Nl & \frac{2}{15}Nl \end{bmatrix} \tag{20b}$$

We can again draw an important conclusion. The matrix $\boldsymbol{S}_\varepsilon$ has one component part in which the stiffness data do not occur, and the other part is the same matrix that would have been found for $\boldsymbol{S}_\varepsilon$ in the linear theory.

On working out the integrals contained in (20a) for constant EA and EI we shall in fact precisely arrive at the matrix in (3).

With (19) the equation (9) now becomes:

$$\boldsymbol{S}^e = \boldsymbol{C}^T(\boldsymbol{S}_\varepsilon^0 + \boldsymbol{S}_\varepsilon^n))\boldsymbol{C} + \Delta\boldsymbol{S}^n \tag{21}$$

Writing $\Delta\boldsymbol{S}^{nn}$ to denote all the parts dependent on N we obtain:

$$\Delta\boldsymbol{S}^{nn} = \boldsymbol{C}^T\boldsymbol{S}_\varepsilon^n\boldsymbol{C} + \Delta\boldsymbol{S}^n \tag{22}$$

and (21) thus becomes:

$$\boxed{\boldsymbol{S}^e = \boldsymbol{C}^T\boldsymbol{S}_\varepsilon^0\boldsymbol{C} + \Delta\boldsymbol{S}^{nn}} \tag{23}$$

We see that the assumption of a displacement field results in an uncoupling of the material non-linearity and the geometric non-linearity. This latter is entirely taken into account with an additional matrix $\Delta\boldsymbol{S}^{nn}$. The material non-linearity affects only the three-by-three matrix $\boldsymbol{S}_\varepsilon^0$ which is valid also in the linear theory.

On now proceeding to consider cracking and plastification, i.e., the cases where $y_z \neq 0$, we need only investigate how S_ε^0 is altered. As the strains are the derivatives of the displacements, we shall first take a closer look at these. The choice of (15) means that for the displacement $u(x, \bar{y})$ at a distance $\bar{y}$ from the centroidal axis the following expression holds:

$$u(x, \bar{y}) = \bar{u}(x) - \bar{y}\frac{dv}{dx} \tag{24}$$

For a line extending parallel to the centroidal axis at some distance therefrom $\bar{y}$ is constant, so that there a quadratic course for $u(x, \bar{y})$ is possible. We shall wish to choose as our axis for the member such a line which does not coincide with the centroidal axis, and we must therefore make an assumption as to the functional behaviour of $u(x)$ and $v(x)$ in that line (Fig. 9b).

At a distance y from this axis of the member the horizontal displacement is:

$$u(x, y) = u(x) - y\frac{dv}{dx} \tag{25}$$

At the actual axis of the member the distance y is zero, so that there $u(x)$ must describe the displacement alone. We have shown that the function for this will be at least quadratic. We shall accordingly decide to choose a *second-degree* interpolation for $u(x)$ at the axis of the member. The three displacement parameters adopted for the purpose are indicated in Fig. 10a. At the intermediate node the *additional* displacement in relation to a linear function is treated as the unknown. As will appear in due course, we thus obtain the best tie-up with the existing programs.

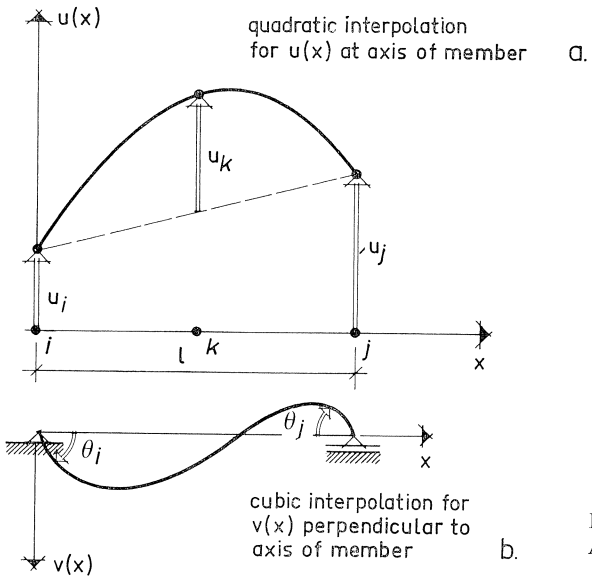

Fig. 10.
Assumed displacement field.

The third-degree interpolation for $v(x)$ remains valid irrespective of the position of the x-axis (Fig. 10b). Our displacement field is therefore determined by:

$$u(x) = \frac{l-x}{l} u_i + \frac{x}{l} u_j + \frac{4x(l-x)}{l^2} u_k \tag{26}$$

$$v(x) = \frac{x(l-x)^2}{l^2} \theta_i + \frac{-x^2(l-x)}{l^2} \theta_j$$

At the axis of the member we may again consider an average strain ε_g and the curvature $\varkappa$ (Fig. 9b). The relation with $u(x)$ and $v(x)$ follows directly from (26):

$$\varepsilon_g = \frac{du}{dx} = \frac{\Delta l}{l} + \frac{4l-8x}{l^2} u_k$$

$$\varkappa = -\frac{d^2 v}{dx^2} = \frac{4l-6x}{l^2} \theta_i + \frac{2l-6x}{l^2} \theta_j \tag{27}$$

The deformation part $\frac{1}{2}(EA\bar{\varepsilon}_g^2 + EI\varkappa^2)$ of the potential energy P as given by (17) (still expressed in $\bar{\varepsilon}_g$ and $\varkappa$) is written as follows in matrix notation:

$$\tfrac{1}{2}[\bar{\varepsilon}_g \quad \varkappa] \begin{bmatrix} EA & 0 \\ 0 & EI \end{bmatrix} \begin{bmatrix} \bar{\varepsilon}_g \\ \varkappa \end{bmatrix} \tag{28}$$

With the relation readily deducible from Fig. 9

$$\bar{\varepsilon}_g = \varepsilon_g + y_z \varkappa$$

the deformation part (28) becomes:

$$\tfrac{1}{2}[\varepsilon_g \varkappa] \begin{bmatrix} D_{11} & D_{12} \\ D_{21} & D_{22} \end{bmatrix} \begin{bmatrix} \varepsilon_g \\ \varkappa \end{bmatrix} \tag{29}$$

where:

$$D_{11} = EA$$
$$D_{21} = y_z EA$$
$$D_{12} = D_{21}$$
$$D_{22} = EI + y_z^2 EA$$

The equation (14) expressed the relation between the quantities $\bar{\varepsilon}_g$, $\varkappa$, N and $\overline{M}$ as defined at the centroidal axis. Thus the matrix $\boldsymbol{D}$ from (29) now expresses the relation between ε_g, $\varkappa$, N and M at the chosen axis of the member.

The procedure of minimalising P follows the same further pattern as before. We now use (27) and (29), so that we obtain four equations comprising u_k, Δl, θ_i and θ_j.

$$
\begin{bmatrix} S_{11} & S_{12} & S_{13} & S_{14} \\ & S_{22} & S_{23} & S_{24} \\ & & S_{33} & S_{34} \\ \text{symmetric} & & & S_{44} \end{bmatrix} \begin{bmatrix} u_k \\ \Delta l \\ \theta_i \\ \theta_j \end{bmatrix} = \begin{bmatrix} 0 \\ N \\ M_i \\ M_j \end{bmatrix} \tag{30}
$$

The terms S_{mn} of the matrix $\boldsymbol{S}$ are integrals which are simple to work out, as in (20a), while the terms of the $\boldsymbol{D}$ matrix take the place of EA and EI. With $\psi = x/l$ the terms are:

$$
\begin{aligned}
S_{11} &= \frac{1}{l}\int_0^1 (4-8\psi)^2 D_{11}\,\mathrm{d}\psi \\
S_{12} &= \frac{1}{l}\int_0^1 (4-8\psi) D_{11}\,\mathrm{d}\psi \\
S_{13} &= \frac{1}{l}\int_0^1 (4-8\psi)(4-6\psi) D_{12}\,\mathrm{d}\psi \\
S_{14} &= \frac{1}{l}\int_0^1 (4-8\psi)(2-6\psi) D_{12}\,\mathrm{d}\psi \\
S_{22} &= \frac{1}{l}\int_0^1 D_{11}\,\mathrm{d}\psi \\
S_{23} &= \frac{1}{l}\int_0^1 (4-6\psi) D_{12}\,\mathrm{d}\psi \\
S_{24} &= \frac{1}{l}\int_0^1 (2-6\psi) D_{12}\,\mathrm{d}\psi \\
S_{33} &= \frac{1}{l}\int_0^1 (4-6\psi)^2 D_{22}\,\mathrm{d}\psi \\
S_{34} &= \frac{1}{l}\int_0^1 (2-6\psi)(4-6\psi) D_{22}\,\mathrm{d}\psi \\
S_{44} &= \frac{1}{l}\int_0^1 (2-6\psi)^2 D_{22}\,\mathrm{d}\psi
\end{aligned} \tag{31}
$$

For (30) we can write the more compact expression:

$$
\begin{bmatrix} \boldsymbol{S}_{uu} & \boldsymbol{S}_{u\varepsilon} \\ \boldsymbol{S}_{\varepsilon u} & \boldsymbol{S}_{\varepsilon\varepsilon} \end{bmatrix} \begin{bmatrix} \boldsymbol{u} \\ \boldsymbol{v}_\varepsilon \end{bmatrix} = \begin{bmatrix} \boldsymbol{0} \\ \boldsymbol{k}_\varepsilon \end{bmatrix} \tag{32}
$$

Here the vector $\boldsymbol{u}$ is the parameter u_k, and $\boldsymbol{v}_\varepsilon$ contains Δl, θ_i and θ_j. There are actually two equations stated in (32). From the first of these we can derive a relation between

$\boldsymbol{u}$ and $\boldsymbol{v}_\varepsilon$. We can then introduce this relation into the second equation, which thereby becomes:

$$[\boldsymbol{S}_{\varepsilon\varepsilon} - \boldsymbol{S}_{\varepsilon u}\boldsymbol{S}_{uu}^{-1}\boldsymbol{S}_{u\varepsilon}]\,\boldsymbol{v}_\varepsilon = \boldsymbol{k}_\varepsilon \tag{33}$$

The matrix between square brackets is the required three-by-three stiffness matrix $\boldsymbol{S}_\varepsilon^0$ for an arbitrary distribution of the stiffness E.

The displacement u_k can be calculated from $\boldsymbol{v}_\varepsilon$ according to the first equation of (30):

$$u_k = -\frac{S_{12}}{S_{11}}\Delta l - \frac{S_{13}}{S_{11}}\theta_i - \frac{S_{14}}{S_{11}}\theta_j \tag{34}$$

Finite difference technique

In the approach based on the finite difference method a series of equidistant points along the member is considered. There are m such points between the ends i and j. At all the points we know EA, EI and the distance y_z from the centroid to the chosen axis of the member. The matrix $\boldsymbol{F}$ of influence coefficients can be determined by a simple procedure. From this we obtain the matrix $\boldsymbol{S}_\varepsilon$ by inversion. The calculation of the three-by-three matrix $\boldsymbol{F}$ is performed as follows. First, we apply at the axis of the member a normal force of unit magnitude. We calculate how much the distance between point i and point j is increased (F_{11}) and how much node i and node j rotate (F_{12} and F_{13}). Next, we consider the case where a unit moment acts at node i; again we calculate the corresponding three deformations: F_{21}, F_{22} and F_{23}. Finally, we perform a similar calculation for a unit moment acting at node j, so that we obtain F_{31}, F_{32} and F_{33}.

In each of these three loading cases we first calculate the extension of the actual centroidal axis and the rotations at the ends thereof. The extension of the axis of the member then follows directly from this by means of a simple transformation. The rotations at the nodes i and j are equal to those which occur at the ends of the centroidal axis.

The change in length of the centroidal axis occurs only in the case where the normal force of unit magnitude is acting. This change in length is then:

$$\int_0^l \frac{1}{EA}\,\mathrm{d}x \tag{35}$$

The integration is performed numerically. In general, the rotations of the ends of the centroidal axis occur in all the three above-mentioned unit cases. In the first case the external moment M_u is equal to the product of the eccentricity y_z and the normal force of unit magnitude. In the second and the third case the external moment M_u varies linearly from unity to zero. The differential equation for the deflection v of the centroidal axis is as follows (N is positive if it is a tensile force):

$$-EI\frac{d^2v}{dx^2} + Nv = M_u \tag{36}$$

At the m difference points we shall consider the discrete values of v as unknowns. At each point p there is a known value EI_p and a known value M_{up}; let h denote the spacing of the points. At such a point we can now write for (36):

$$-v_{p-1} + \left[2 + \frac{Nh^2}{EI_p}\right]v_p - v_{p+1} = \frac{h^2}{EI_p}M_{up} \tag{37}$$

For N we substitute the value that we expect to obtain as the result. In an iteration process each successive stage is performed with the result yielded by the preceding calculation. Equation (37) is established for all m difference points. For v at node i and node j a zero value is introduced. We obtain a set of equations comprising m unknowns v; the matrix of the coefficients is symmetric and has a pronounced banded structure. The rotations follow from the solution of the set of equations:

$$\begin{aligned} \theta_i &= \frac{v_1}{h} + \frac{h}{2EI_i}M_i \\ \theta_j &= -\frac{v_m}{h} + \frac{h}{2EI_j}M_j \end{aligned} \tag{38}$$

In this way a completely symmetric matrix $\boldsymbol{F}$ is established, so that $\boldsymbol{S}_\varepsilon$ will also display pure symmetry. There is a significant difference in relation to the method based on an assumed displacement field. With the finite difference technique it is not possible to uncouple the material and the geometric non-linearity. We obtain the matrix $\boldsymbol{S}_\varepsilon$ "at one go". The separation into $\boldsymbol{S}_\varepsilon^0$ and $\boldsymbol{S}_\varepsilon^n$ can now not be done.

The six-by-six matrix $\boldsymbol{S}^e$ therefore follows directly from (compare with 23):

$$\boxed{\boldsymbol{S}^e = \boldsymbol{C}^T\boldsymbol{S}_\varepsilon\boldsymbol{C} + \Delta\boldsymbol{S}^n}$$

In Section 6 we shall confine ourselves to the "assumed deflected shape" method. The reader can verify for himself how, on similar lines, the problem can alternatively be dealt with by the finite difference technique.

6 How the program works

General

In principle, a non-linear analysis proceeds as indicated in Fig. 11. We choose an initial estimated value for the normal forces N and the magnitude of the modulus of elasticity E. For N this value is zero, and for E we adopt the value at the origin of the stress-strain diagram.

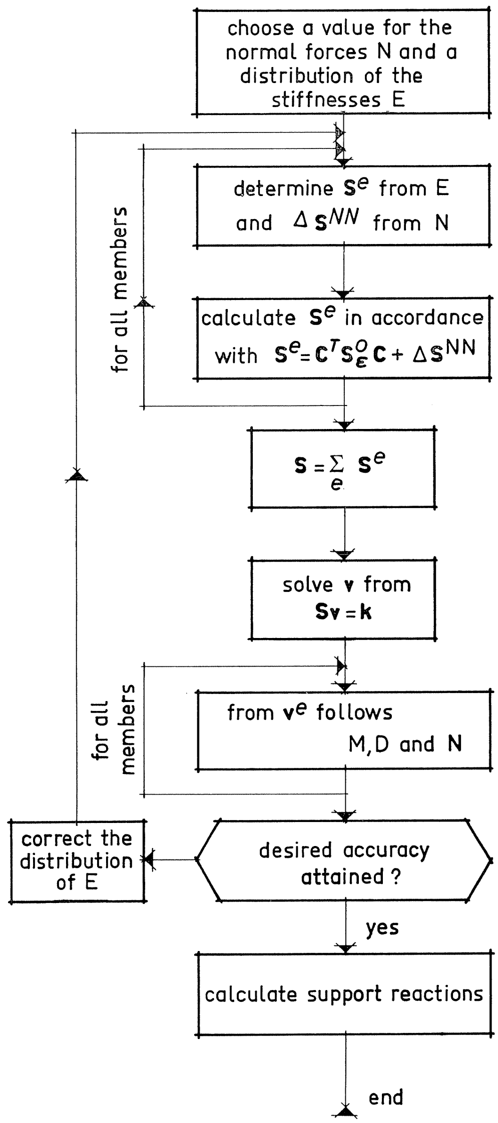

Fig. 11.
Approximate flowchart for a non-linear analysis of framed structures.

For each member of the structure we choose an axis (the axis of that member), after which S^0_ε can be calculated in accordance with (33) and S^{nn} can be calculated with (22). The total matrix S^e is then obtained from (23). The further procedure is the same as that for a program based on the linear theory. When finally v^e and N for all the members are known, the calculation can be repeated with a better estimated value for S^e.

With v^e the values of u_i, u_j, u_k, θ_i and θ_j respectively are definitely established, and therefore with (27) the average strain ε_g and the curvature $\varkappa$ at each section of the member is likewise established. The total strain across the depth of each section is then known (see Fig. 9b). The apparent E associated with this strain can then be red from the σ–ε diagram of the material. This operation of seeking the value of E corresponding to a particular strain ε will always have to be performed, whatever the shape and constitution of the section, and is the only stage in the analysis procedure at which the chosen σ–ε-diagram comes into it. As stated earlier on, this part is accommodated in a separate subroutine (EMOD). The input parameter is the strain and the output parameter is the required E.

From the new distribution for E the two-by-two matrix $\boldsymbol{D}$ can be calculated with (13) and (29). This matrix $\boldsymbol{D}$ is typically determined by the shape and constitution of the cross-section of the member and is accordingly produced in a subroutine (DRSN) already referred to. For each cross-sectional shape an individual DRSN subroutine will have to be established. The input parameters are ε_g and $\varkappa$; the output parameters are the terms D_{11}, D_{12} and D_{22}. In the DRSN subroutine a call is made upon the EMOD subroutine for determining the apparent moduli of elasticity E. The integrations in (31) are performed numerically with the aid of the trapezoidal rule.

The final step consists in calculating the matrix $\boldsymbol{S}_{\varepsilon}^{0}$ for the member from (30), (32) and (33). The calculated matrices $\boldsymbol{D}$ are used for the purpose. Now an integration over the length of the member has to be performed. Simpson's rule is applied here, as greater accuracy is desirable. For an elastic prismatic member the exact stiffness matrix will then in any case be obtained. Determining the stiffness terms of $\boldsymbol{S}_{\varepsilon}^{0}$ is performed in a subroutine (STYTER). In principle, this subroutine need be programmed only once and is at the disposal of all users. It will have to be altered only if it is felt nessecary in future to assume another displacement field.

STANIL program

On the basis of the "philosophy" outlined above, the Data Processing Division (Dienst Informatieverwerking) of the Rijkswaterstaat has prepared a program designated as STANIL, which is made available also to other users. For this purpose a program for the analysis of plane framed structures which was already at the disposal of that Division has been modified somewhat. As already stated, this involves mainly the writing of the three subroutines EMOD, DRSN and STYTER. The FORTRAN lists of these routines are appended to this paper. Any one who has a normal program at his disposal can apply the modifications quite simply. The STYTER subroutine will, in principle, always remain valid; EMOD will have to be changed only if the C.E.B. (European Committee for Concrete) sees fit to revise the recommended stress-strain diagrams, and DRSN will have to be individually established for each cross-sectional shape (and is independent of the material properties). The program obtained really is very general. Merely by altering EMOD it can be used also for other materials, such as aluminium, wood, etc.

Example and indication of cost

For eccentrically loaded individual reinforced concrete columns De Groot has in-

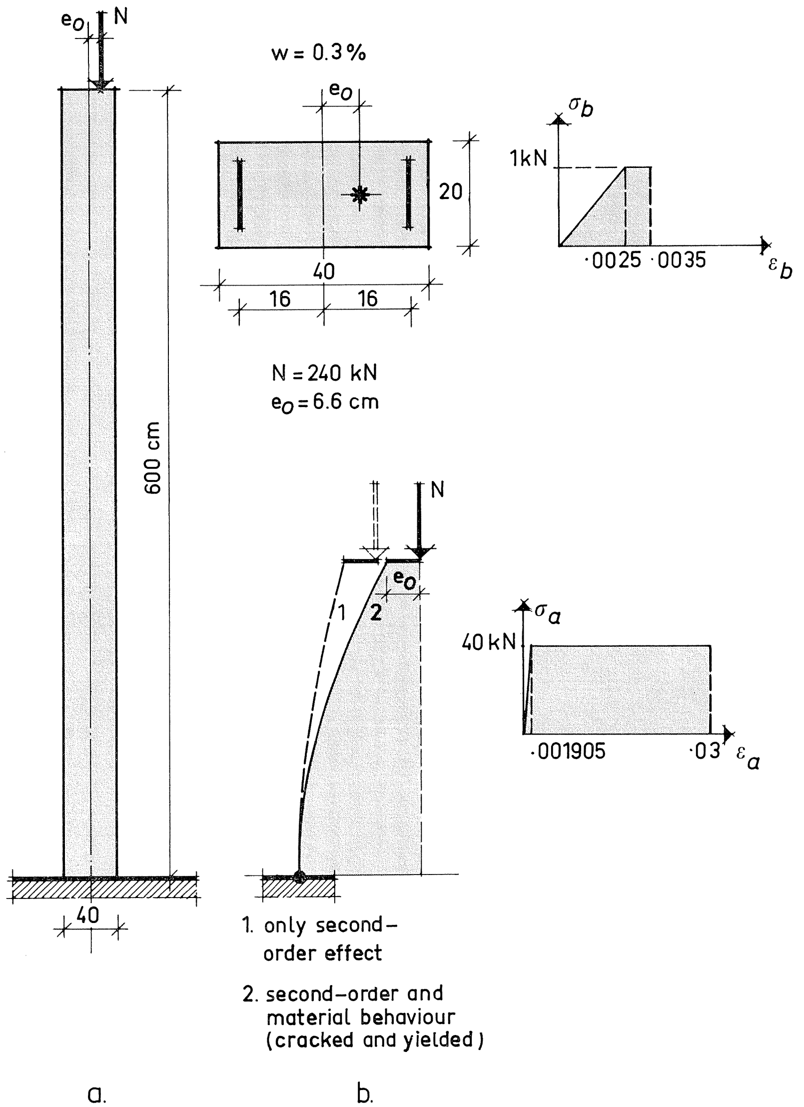

Fig. 12. State of failure of a reinforced concrete column.

vestigated a number of cases with the aid of the finite difference technique. One such instance is represented in Fig. 12a. The STANIL program gives practically the same result. For equal eccentricity e_0 the failure load differs by less than $\frac{1}{2}$ per cent from the result obtained by means of the finite difference technique which here is considered to be the exact one. In this comparison the column comprises one element. In Fig. 12b it is shown how the displacement increases in consequence of cracking in the concrete. Because of this the largest moment increases by about 50% in relation to the uncracked state. In actual calculations for the analysis of frameworks similar results may be obtained. No examples of such cases will be given here, but we shall, in conclusion, give some idea of the cost of performing such calculations. A framed system comprising 183 joints (nodes) and 240 members of seven different types, largest node number difference of 10, attains equilibrium after four iterations, for a given loading. The cost of performing the analysis on the CDC6600 computer is approximately Fl. 85.— ($ 25.—).

7 Concluding remarks

It is possible to fulfil in a simple manner the desired features listed in Section 2 of this paper. Interchangeability of a quite unexpected simplicity has been achieved. The most important task to be performed consists in writing the DRSN subroutine for the cross-sectional shapes currently used in structural engineering practice. The DRSN for rectangular sections is given in an appendix to this paper.

The present author hopes that others will write and publish DRSN subroutines for T-beams, round columns, square box-shaped members (e.g., as embodied in the structural cores of tall buildings), etc. It should thus be possible to avoid unnescessary duplication of work by engineers all individually producing their own programs.

It is alternatively possible to apply the finite difference technique. For this the STYTER subroutine will have to be somewhat modified, but otherwise the scheme presented here remains applicable.

Finally, it should be noted that the method can also be so formulated that the analysis can be performed with increments of the loading. In that case it is not necessary to use an apparent modulus of elasticity; the tangent modulus can be introduced instead. This may be advantageous if it is desired to investigate accurately the formation of concentrated ideally plastic hinges.

Translator's note:

The acronyms used to denote the subroutines and programs are based on Dutch words:
DRSN is derived from "*d*oo*rs*n*ede" = "section" (of a structural member)
EMOD is derived from "*e*lasticiteits*mod*ulus" = "modulus of elasticity"
STYTER is derived from "*sty*fheids*ter*men" = "stiffness terms"
STANIL is derived from "*sta*afconstructies *ni*et-*l*ineair" = "non-linear framed structures".

```
      SUBROUTINE STYTER(S11,S12,S13,S22,S23,S33,C1,C2,C3)
C
C     THE SUBROUTINE DETERMINES THE THREE-BY-THREE STIFFNESS MATRIX
C     OF A MEMBER BY MEANS OF NUMERICAL INTEGRATION. THE THREE-
C     BY-THREE STIFFNESS MATRIX RELATES TO THE THREE DEFORMATIONS
C     DELTAL, TET1 AND TET2. THE ROUTINE STARTS FROM A MEMBER
C     WHICH IS DIVIDED INTO A NUMBER (NMOT) OF SEGMENTS. PER
C     SEGMENT THE CROSS-SECTIONAL SHAPE MAY BE DIFFERENT.
C     THIS PROVISION HAS BEEN MADE BECAUSE, INTER ALIA, THE
C     REINFORCEMENT MAY VARY WITHIN ONE AND THE SAME MEMBER.
C     THE LENGTHS OF THE SEGMENTS ARE GIVEN IN AN ARRAY ALMOT.
C     PER SEGMENT AN EQUIDISTANT DIVISION INTO STEPS IS MADE.
C     THE NUMBER OF STEPS PER SEGMENT IS EVEN, SO AS TO ENABLE
C     INTEGRATION TO BE PERFORMED PER SEGMENT WITH SIMPSON≠S RULE.
C     THE NUMBER OF STEPS FOR THE VARIOUS SEGMENTS OF A MEMBER IS
C     PASSED IN AN ARRAY NSTMOT FROM THE MAIN PROGRAM TO THIS
C     SUBROUTINE. HOW THIS NUMBER IS ESTABLISHED IN MAIN IS NOT
C     OF IMPORTANCE HERE. IT MAY DIFFER FROM ONE PROGRAM TO
C     ANOTHER.
C     PER SEGMENT THE NUMBER OF SECTIONS CONSIDERED IS ONE MORE
C     THAN THE NUMBER OF STEPS. THE STIFFNESS NUMBERS D11, D21 AND
C     D22 OF ALL THE SECTIONS OF ALL THE SEGMENTS OF THE MEMBER ARE
C     ARRANGED IN SEQUENCE IN THE THREE ARRAYS DD11, DD21 AND DD22.
C     THE SIX TERMS OF THE UPPER TRIANGLE OF THE STIFFNESS MATRIX
C     ARE S11, S12, S13, S22, S23 AND S33.
C     THE THREE COEFFICIENTS C1, C2 AND C3 CAN BE USED FOR
C     CALCULATING THE HORIZONTAL DISPLACEMENT UK HALFWAY ALONG THE
C     MEMBER FROM DELTAL, TET1 AND TET2. THE RELATION IS:
C     UK= C1*DELTAL + C2*TET1 + C3*TET2
C     IN THE CHOICE OF THE ARRAY DIMENSIONS IT IS ASSUMED THAT
C     THERE ARE UP TO 5 SEGMENTS PER MEMBER AND AN AVERAGE OF 5
C     SECTIONS PER SEGMENT (MAXIMUM 25 SECTIONS). THE ARRAYS
C     SO, Y AND S ARE AUXILIARY ARRAYS. THE ARRAY VUL IN COMMON
C     RELATES TO DATA WHICH ARE NOT USED IN STYTER.
C
      DIMENSION SO(10),Y(10,25),S(10)
      COMMON VUL(16),DD11(25),DD21(25),DD22(25),NMOT,ALMOT(5),NSTMOT(5)
      X1=0
      NN=0
      DO 10 J=1,10
      S(J)=0.
   10 CONTINUE
      AL=0.
      DO 20 L=1,NMOT
      AL=AL+ALMOT(L)
   20 CONTINUE
      DO 290 L=1,NMOT
      AL1=ALMOT(L)
      N=NSTMOT(L)
      AL3=AL1/(3*N*AL*AL)
      FN=N
      X=AL1/(FN*AL)
      X1=X1-X
      N1=N+1
      DO 100 I=1,N1
      NN=NN+1
      X1=X1+X
      Z1=DD11(NN)
      Z2=DD21(NN)
      Z3=DD22(NN)
      A1=6*X1
      A2=24*X1
      A3=36*X1
      B1=X1*X1
      B2=36*B1
      B3=48*B1
      Y(1,I)=Z1
      Y(2,I)=(-A1+4)*Z2
      Y(3,I)=(-A1+2)*Z2
      Y(4,I)=(B2-2*A2+16)*Z3
      Y(5,I)=(B2-A3+8)*Z3
      Y(6,I)=(B2-A2+4)*Z3
      Y(7,I)=(64*B1-64*X1+16)*Z1
      Y(8,I)=(4-8*X1)*Z1
      Y(9,I)=(B3-56*X1+16)*Z2
      Y(10,I)=(B3-40*X1+8)*Z2
  100 CONTINUE
      DO 101 J=1,10
  101 SO(J)=0
      DO 250 J=1,10
      DO 200  I=2,N,2
      OP=Y(J,I-1)+4*Y(J,I)+Y(J,I+1)
  200 SO(J)=SO(J)+OP*AL3
  250 CONTINUE
      DO 260  J=1,10
      S(J)=S(J)+SO(J)
  260 CONTINUE
  290 CONTINUE
      S7=S(7)
      S8=S(8)
      S9=S(9)
      S0=S(10)
      S11=S(1)-S8*S8/S7
      S12=S(2)-S8*S9/S7
      S13=S(3)-S8*S0/S7
      S22=S(4)-S9*S9/S7
      S23=S(5)-S9*S0/S7
      S33=S(6)-S0*S0/S7
      C1=-S8/S7
      C2=-S9/S7
      C3=-S0/S7
      RETURN
      END
```

```
      SUBROUTINE  DRSN(EG,SKAP,D11,D21,D22)
C
C     THE CROSS-SECTION IS RECTANGULAR WITH
C     TOP AND BOTTOM REINFORCEMENT. THE
C     AVERAGE STRAIN EG AND THE CURVATURE SKAP
C     ENTER INTO THE SUBROUTINE. THE OUTPUT
C     CONSISTS OF THE THREE STIFFNESS NUMBERS
C     D11, D21 AND D22. THE DEPTH OF THE
C     SECTION IS DIVIDED INTO N INTEGRATION
C     STEPS. THE CONCRETE STRAIN IS
C     DETERMINED AT NB=N+1 POINTS AND THE STEEL
C     STRAIN AT NS=2 POINTS.
C     THE STRAINS OCCUR IN THIS SEQUENCE IN THE
C     ARRAY EPS. THE CORRESPONDING MODULI OF
C     ELASTICITY E ARE DETERMINED IN THE EMOD
C     SUBROUTINE. THESE FORM THE BASIS FOR THE
C     CALCULATION OF D11, D21 AND D22.
C     IN THE COMMON AREA ARE:
C     VUL(6)     = DATA WHICH ARE NOT USED IN
C                  DRSN (SEE EMOD)
C     IFOUTS     = COUNTER FOR SIGNALLING (SEE
C                  EMOD)
C     IFOUTB     = DITTO
C     H1         = DISTANCE FROM BOTTOM CONCRETE
C                  FIBRE TO AXIS OF MEMBER
C     H2         = DITTO FROM TOP CONCRETE FIBRE
C                  (GIVE AS NEGATIVE)
C     E1         = DISTANCE FROM BOTTOM
C                  REINFORCEMENT TO AXIS OF MEMBER
C     E2         = DITTO FROM TOP REINFORCEMENT
C                  (GIVE AS NEGATIVE)
C     W1         = BOTTOM REINFORCEMENT
C                  PERCENTAGE (POSITIVE)
C     W2         = TOP REINFORCEMENT PERCENTAGE
C                  (POSITIVE)
C     BR         = WIDTH OF SECTION
C     N          = NUMBER OF STEPS FOR THE
C                  TRAPEZOIDAL RULE
C     THE ARRAY SIG IS AN AUXILLIARY ARRAY.
C
      COMMON VUL(6),IFOUTS,IFOUTB,H1,H2,E1,E2,W1,
      DIMENSION EPS(15),ELA(15),SIG(15)
      TOTH=H1-H2
      AFST=TOTH/N
      HAF=AFST/2
      NS=2
      NB=N+1
      NK=NB
      HW1=W1*TOTH/100.
      HW2=W2*TOTH/100.
C     CALCULATION OF TOTAL STRAIN DISTRIBUTION
      DO 1 I=1,NK
    1 EPS(I)=EG+SKAP*(H2+(I-1)*AFST)
      EPS(NK+1)=EG+SKAP*E1
      EPS(NK+2)=EG+SKAP*E2
      CALL EMOD (EPS,ELA,NB,NS)
      ELS1=ELA(NK+1)
      ELS2=ELA(NK+2)
C     CALCULATION OF D11, D21 AND D22
      D11=0
      D21=0
      D22=0
      DO 2 I=1,NK
    2 SIG(I)=ELA(I)*(H2+(I-1)*AFST)
      DO 5 I=1,N
      X1=ELA(I)
      X2=ELA(I+1)
      X3=SIG(I)
      X4=SIG(I+1)
      A=HAF*(X1+X2)
      XH=H2+AFST*I
      XG=XH-2./3.*AFST
      B=HAF*X1*XG
      C=HAF*X3*XG
      XG=XH-1./3.*AFST
      B=B+HAF*X2*XG
      C=C+HAF*X4*XG
      D11=D11+A
      D21=D21+B
      D22=D22+C
    5 CONTINUE
      AST2=HW2*ELS2
      AST1=HW1*ELS1
      D11=D11     +AST2+AST1
      D21=D21     +E2*AST2+E1*AST1
      E222=E2*E2*AST2
      E223=E1*E1*AST1
      D22=D22+E222+E223
      D11=D11*BR
      D21=D21*BR
      D22=D22*BR
      RETURN
      END
```

```
      SUBROUTINE  EMOD(EPS,ELA,NB,NS)
C
C     NB + NS STRAINS ENTER INTO THE ARRAY
C     EPS. THE MODULUS OF ELASTICITY
C     SELECTED AS CORRESPONDING TO THESE
C     IS IN TURN GIVEN OUT IN THE ARRAY
C     ELA. THE FIRST NB POSITIONS RELATE
C     TO CONCRETE AND THE FOLLOWING NS
C     RELATE TO STEEL. THE SIGMA-EPSILON
C     DIAGRAM OF BOTH THE CONCRETE AND
C     THE STEEL IS BILINEAR. THE CONCRETE
C     CANNOT RESIST TENSION
C     IN THE COMMON AREA ARE:
C     SVLS    = YIELD STRESS OF STEEL
C     SVLB    = YIELD STRESS OF CONCRETE
C     ES1     = STEEL STRAIN AT START OF
C               YIELDING
C     ES2     = FAILURE STRAIN OF STEEL
C     EB1     = CONCRETE STRAIN AT START
C               OF YIELDING
C     EB2     = FAILURE STRAIN OF CONCRETE
C     IFOUTS = COUNTER; THIS IS INCREASED
C               BY ONE UNIT IF EBS2 IS
C               ANYWHERE EXCEEDED
C     IFOUTB = DITTO FOR EB2
C     THESE COUNTERS ARE USED FOR
C     SIGNALLING(FLAGS).
C
      COMMON SVLS,SVLB,ES1,ES2,EB1,EB2,
     *IFOUTS,IFOUTB
      DIMENSION ELA(15),EPS(15)
      NK2=NB+NS
      DO 1 I=1,NK2
      IF (EPS(I)) 2,2,3
    3 ELA(I)=0
      GO TO 1
    2 EPS(I)=ABS(EPS(I))
      IF (EPS(I)-EB1) 5,5,4
    5 ELA(I)=SVLB/EB1
      GO TO 1
    4 IF (EPS(I)-EB2) 7,7,6
    7 ELA(I)=SVLB/EPS(I)
      GO TO 1
    6 CONTINUE
      IFOUTB=IFOUTB+1
    1 CONTINUE
      NK1=NB+1
      DO 20 I=NK1, NK2
      E1=ABS(EPS(I))
      IF(E1-ES1) 11,11,12
   11 ELA(I)=SVLS/ES1-ELA(I)
      GO TO 20
   12 IF (E1-ES2) 13,13,14
   13 ELA(I)=SVLS/E1-ELA(I)
      GO TO 20
   14 IFOUTS=IFOUTS+1
   20 CONTINUE
      RETURN
      END
```

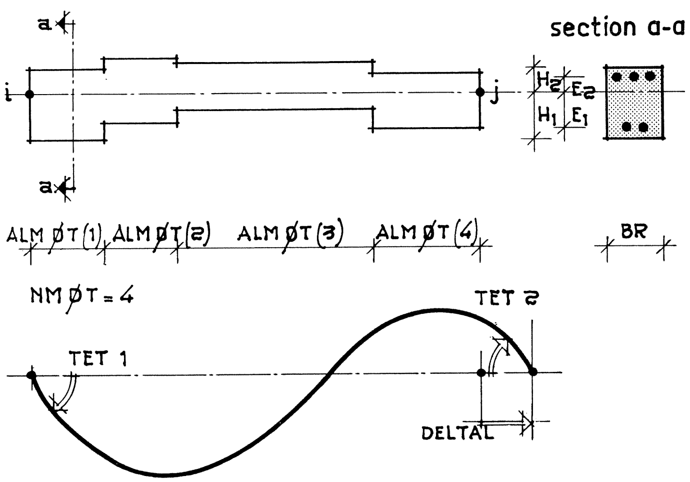

Fig. 13.
Explanation relating to DRSN and STYTER subroutines.

References

1. Livesley, M. A., Matrix Methods of Structural Analysis, 1964.

2. Betonvereniging, Lecture notes for the course "Moderne Rekenhulpmiddelen en Methoden" (Modern computation techniques and methods), Chapter 4: Enkele matrixmethoden voor het berekenen van staafconstructies (Some matrix methods for the analysis of framed structures), by J. Blaauwendraad.*

3. Jennings, A. and K. Majid, An elastic-plastic analysis by computer for framed structures loaded up to collapse. The Structural Engineer, December 1965, No. 12, Vol. 43.

4. Blaauwendraad, J. Moderne rekentechnieken voor stabiliteitsonderzoek (Modern computation techniques for stability analysis). Syllabus of the course on Stability of Buildings (lectures Nos. 10 and 11) of the Stichting Post-Doktoraal Onderwijs in het Bouwen, October 1970.*

5. Leeuwen, J. van and A. C. van Riel, Berekening van centrisch en excentrisch gedrukte constructiedelen volgens de breukmethode (Analysis of axially and eccentrically loaded structural components by the ultimate load method). Heron 10 (1962), No. 3/4.*

6. Groot, A. K. de and A. C. van Riel, De stabiliteit van kolommen en wanden van ongewapend beton (The stability of plain concrete columns and walls). Heron 15 (1967), No. 3/4.*

7. Groot, A. K. de, Rekenmethode voor gewapend-betonkolommen (Method of analysis for reinforced concrete columns). Syllabus of the course on Stability of Buildings of the Stichting Post-Doktoraal Onderwijs in het Bouwen, September 1970 (TNO-IBBC Report B170-62).*

* In Dutch.